POST OXIDE ETCHING CLEANING PROCESS USING INTEGRATED ASHING AND HF VAPOR PROCESS

by

OHSEUNG KWON

B.S. MATERIALS SCIENCE AND ENGINEERING
KOREA INSTITUTE OF SCIENECE AND TECHNOLOGY, 1991

M.S. MATERIALS SCIENCE AND ENGINEERING
KOREA INSTITUTE OF SCIENCE AND TECHNOLOGY, 1993

Submitted to the Department of Materials Science and Engineering in Partial Fulfillment of the Requirements for the Degree of

Master of Science in Materials Science and Engineering

at the
Massachusetts Institute of Technology
June 1999

Signature of Author.....
Department of Materials Science and Engineering
May 7, 1999

Certified by.....
Professor Herbert H. Sawin
Professor of Chemical Engineering
and Electrical Engineering and Computer Science
Thesis Supervisor

Accepted by.....
Professor Linn W. Hobbs
John F. Elliott Professor of Materials
Chairman, Departmental Committee on Graduate Students
Department of Materials Science and Engineering

POST OXIDE ETCHING CLEANING PROCESS USING INTEGRATED ASHING AND HF VAPOR PROCESS

by

OHSEUNG KWON

Submitted to the Department of Materials Science and Engineering
On May 7, 1999
In Partial Fulfillment of the Requirements for the Degree of

Master of Science in Materials Science and Engineering

ABSTRACT

A totally integrated dry cleaning process after oxide etching in fluorocarbon gases was proposed and demonstrated on blanket oxide film and patterned 4" wafers. Oxide etching was performed using Inductively Coupled Plasma(ICP) etcher using 100 % CHF_3 gas. In-situ oxygen plasma and HF vapor were used for cleaning fluorocarbon polymeric contamination formed during oxide etching. This process sequence was performed in a vacuum cluster system in our laboratory. In this apparatus, we have the ability to transfer samples between processing chambers and perform surface analysis at a base pressure in the 10^{-9} torr range. In this manner, we can mimic a clustered process, avoid ambient contamination, and obtain an accurate picture of the evolution of the wafer surface throughout the process sequence. We support our cleaning results with quasi in situ angle resolved X-ray Photoelectron Spectroscopy (XPS).
It was demonstrated that planar surfaces after oxide etching could be cleaned, leaving less than one monolayer of oxygen, fluorine, and carbon on the surface.
The proposed cleaning process was also succesful in removing contamination from both sidewalls and trench bottom in line and space patterned samples.

Thesis Supervisor: Herbert H. Sawin
Title : Professor of Chemical Engineering and Electrical Engineering and Computer Science

Table of Contents

List of Figures

List of Tables

Chapter 1
INTRODUCTION

1.1 Motivation

In microelectronic device fabrication processes, plasma processes using fluorocarbon gas mixture are widely used for etching SiO_2. Polymer by-products are formed in this process and play an important role to improve etch selectivity of SiO_2 to Silicon.[1, 2, 3, 4, 5] On the other hand, these polymers formed inside contact holes and vias can be detrimental to device performance. Cleaning of this polymer has become more and more important as dimension of microelectronic device decreases and small amount of contaminants becomes important issue.

This thesis is intended for a systematic understanding of integrated post etch gas phase cleaning processes.

1.2 High Density Plasma Etching

As feature size of microelectronic device decreases resulting in vias and holes with high aspect ratios, conventional diode type Reactive Ion Etching (RIE) process has became less capable of making desired high aspect ratio anisotropic etching profiles. In conventional diode type RIE, ion energy and plasma density are coupled and cannot be independently controlled. However techniques high etching rate with good selectivity are required more and more. In conventional RIE, high etching rate and anisotropy is achieved by increasing the power input to the plasma to result in high ion energy and directionality. Unfortunately increased ion energy makes the process more physical or

sputter etching reducing chemical nature of the process. Since selectivity is enhanced by chemical nature of the etching, increased physical portion of the process results in loss of selectivity and etch profile control.[6]

Recently, low pressure, high density plasma etching techniques have been developed in the fabrication of Ultra Large Scale Integration (ULSI) devices.[6, 7, 8, 9] Among these are Electron Cyclotron Resonance (ECR) plasma source, Inductively Coupled Plasma (ICP) source, and Helicon source. The advantage of these systems are we can control plasma density and ion energy independently so that we can increase plasma density by about two orders of magnitude with relatively low ion energy. With this techniques, we can achieve fast and directional anisotropic etching with a good selectivity without creating severe damages to the device.

1.3 Contamination and Damage in Plasma Oxide Etching

Figure 1.1 shows a schematic diagram of the contamination and damage after a typical RIE process. As discussed by many researchers[2, 3, 10, 11, 12, 13, 14], polymer film deposited in RIE of oxide process using hydrocarbon gases would be teflon-like and the parameter space where net etching and net deposition can occur can be shown as in figure 1.2. Polymer film formed in etching process plays an important role in enhancing oxide etching selectivity to silicon. Since oxygen is liberated from oxide during etching process, polymer film is deposited preferentially on silicon surface and this hinders silicon etching during the oxide etching process. However, this polymer film has to be removed after oxide etching process because this can increase contact resistance in the contact holes formed by etching process. Oehrlein et al[15] reported that the presence of a

film containing carbon and fluorine after overetch and the thickness of the polymer film is limited to 50Å. They also observed the presence of O rich transition layer between the polymer film and the silicon. This layer was believed that it is because the samples were exposed to the air. Coyle et al [16] reported a Si-C layer located at film/silicon interface, while some others such as Thomas et al[17] did not observe at all.

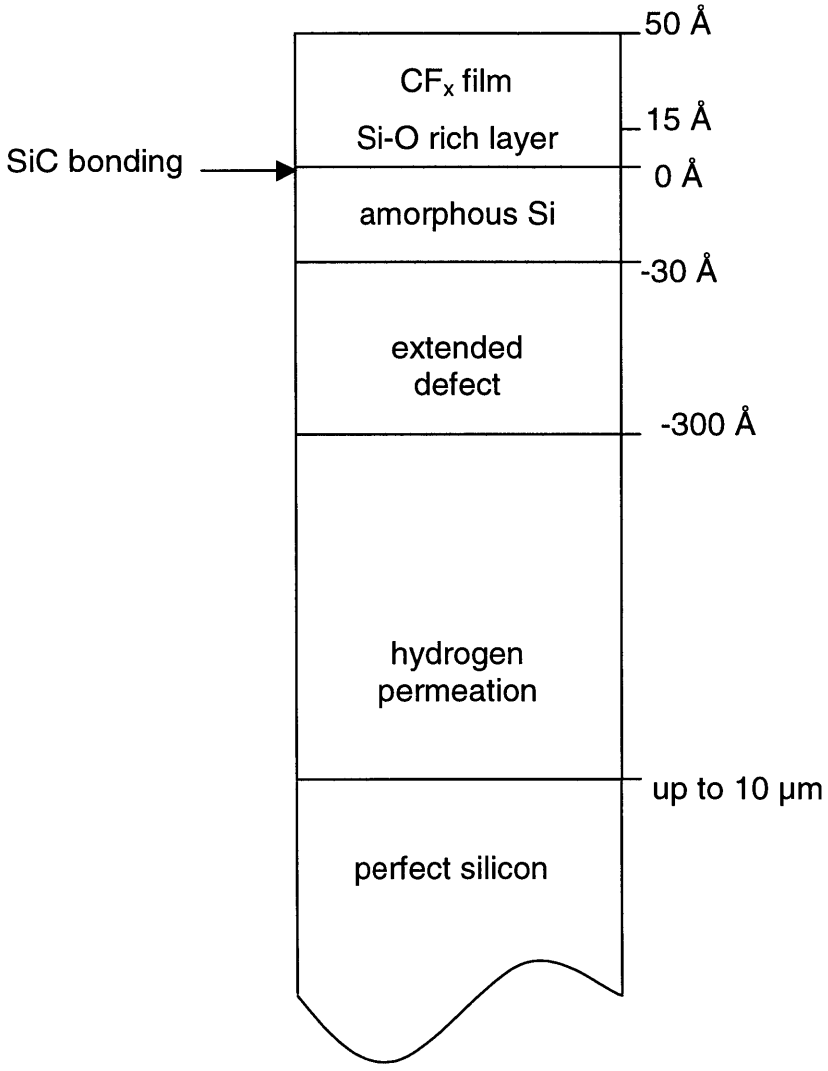

Figure 1.1 A Schematic diagram of contamination and damage after a typical plasma etching process

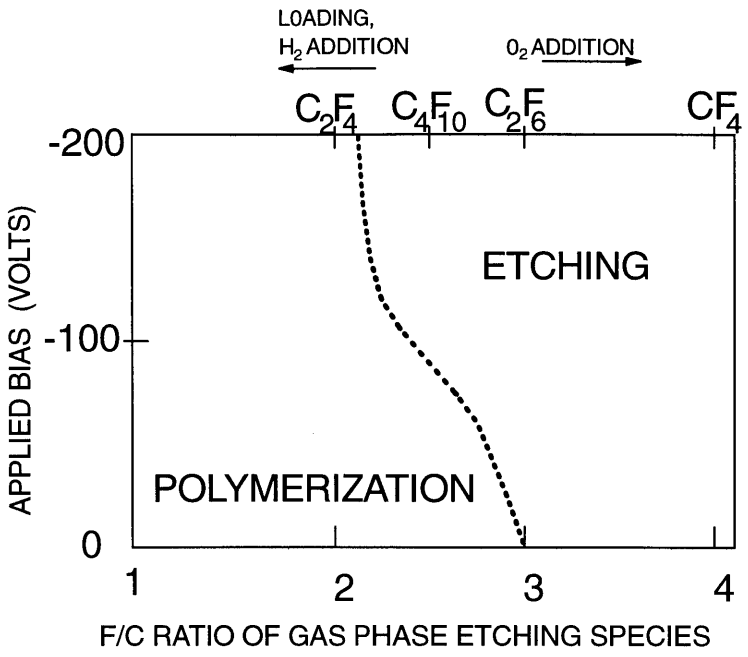

Figure 1.2 Parameter space for etching and deposition in plasma oxide etching and the effect of gas additions. After Coburn et al.[21]

Most of the literature on plasma etching damage and contamination relates to diode type configurations. The contamination and damage induced by Inductively Coupled Plasma (ICP) sources and other high density plasma sources, however, would be quite similar to damage and contamination in diode type configuration. Many research groups such as Oehrlein et al,[2, 3, 18] , Yapsir et al,[19] reported that similar polymer film was formed in high density plasma etching system, with a lower level of substrate damage.

1.4 X-ray Photoelectron Spectroscopy (XPS)

Figure 1.3 is a diagram of the photoelectric process. When a high electron photon with an energy of hν is injected into the sample, an electron absorbs the energy of photon to

produce a photoelectron with an energy of hν -E_b, where E_b is the binding energy of the electron. The energy distribution of photoelectrons directly corresponds to electron energy distribution of the element and the intensity is related to concentration of the element. XPS uses this principle to analyze surface atomic layers of a specimen. The most common X-ray sources are 1486.6eV and 1253.6eV, which are Al K_α and Mg K_α, respectively. Each element has an unique XPS spectrum and a spectrum of a mixture is approximately the sum of spectrums of all the elements in the mixture. Although X-ray can penetrate up to several um into the sample, the escape depth of photoelectron is in the order of 20-50 Å, which makes XPS very useful tool for surface analysis.

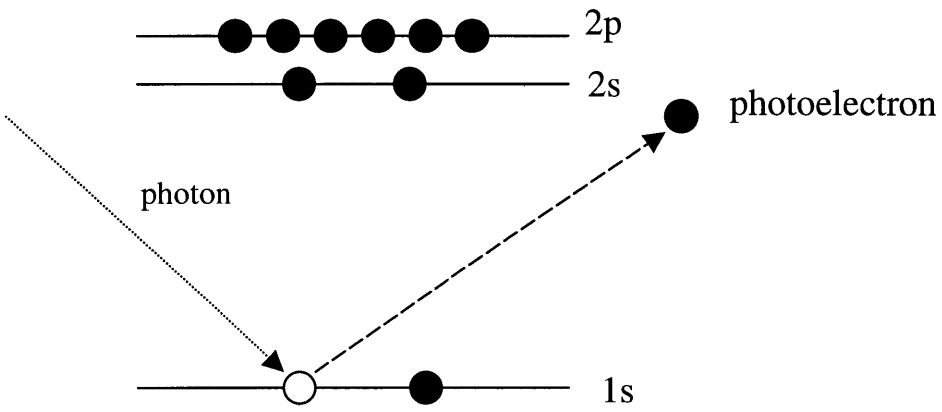

Figure 1.3 Diagram of the photoelectric process

In the presence of chemical bondings, electrons in outer shells are involved in chemical bonding to make changes in energy level of electrons in inner shells. This is called chemical shift. For example binding energy of Si in SiO_2 is 103.4eV, which is 4.25eV higher than in the case of elemental Si.[20] Using this characteristic of XPS, we can

analyze chemical bonding state of each element as well as the composition of the sample. For very small chemical shifts, deconvolution and peak identification has to be done to analyze the peak accurately.

Since XPS is very useful in analyzing electron band structure, oxidation state, chemical bondings, chemisorbed elements, and functional groups in organic compounds, it is often called as ESCA (Electron Spectroscopy for Chemical Analysis).

Chapter 2

EXPERIMENTAL

2.1 Experimental Setup

2.1.1 Integrated Process Apparatus (VAST tube : VAcuum Sample Transfer tube)

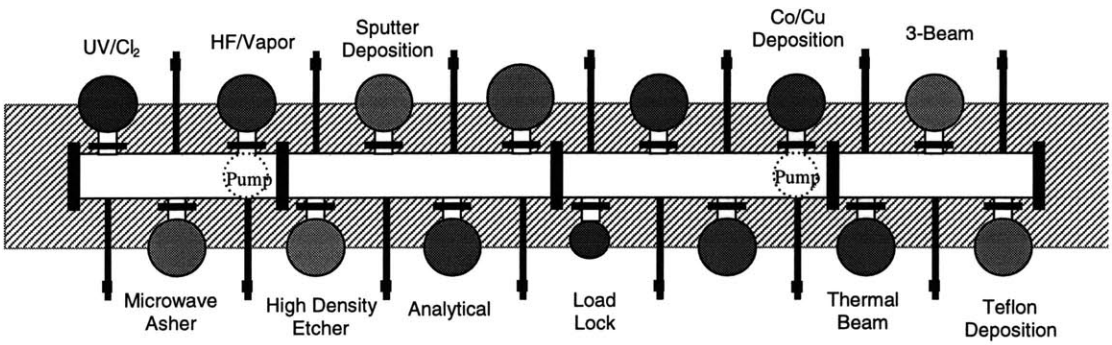

Figure 2.1 A schematic diagram of the Integrated Process Apparatus VAST tube (VAcuum Sample Transfer tube)

Figure 2.1 is a schematic diagram of the integrated processing apparatus. Each processing chamber is connected to the central transfer tube and most of the chambers are capable of processing 4"wafers. In the central transfer tube, a cart is installed to transfer samples along the tube. For loading and removing sample from each processing chamber, transfer rods are used. The transfer tube is maintain in the vacuum of low 10^{-8} to mid 10^{-9}torr, to minimize any contamination during the transfer, allowing us to transfer sample from one processing chamber to another without making sample exposed to the

air. The chambers used in this research were High Density Plasma Etcher, HF Vapor Cleaning Chamber and Analytical Chamber.

2.1.2 Inductively Coupled Plasma (ICP) Etcher

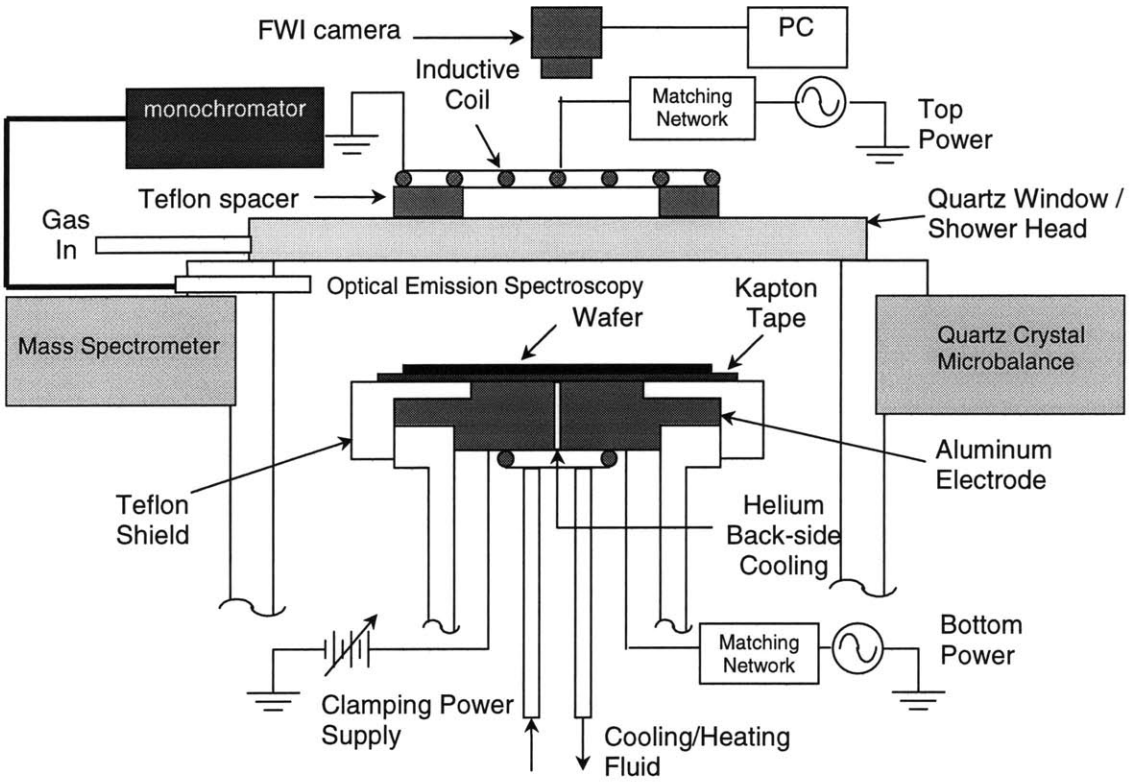

Figure 2.2 A schematic diagram of inductively coupled plasma etcher used in this research

Figure 2.2 shows a schematic diagram of inductively coupled plasma etcher. In this configuration, RF power at 13.56 MHz for generating plasma is supplied to top coil, which is on 0.5" thick quartz window. To reduce capacitive coupling, teflon spacers

were placed between the coil and the quartz window. A separate power is supplied to the substrate to manipulate ion bombarding energy, which is also 13.56 MHz.

The wafer is cooled down by backside cooling water and to enhance thermal contact between the wafer and the electrode electrostatic chuck(ECS) is used with 5 mTorr He backside cooling.

This processing chamber has several diagnostic tools. Charge Coupled Device (CCD) camera is installed to monitor inteferometric signal coming from the sample to monitor etch rate and uniformity. Quartz Crystal Microbalance (QCM) is for investigating angle dependency of the etch rate, Mass Spectroscopy is for analyzing gas composition of the chamber. Langmuir probe characterizes plasma parameters.

2.1.3 HF Vapor Cleaning Chamber

The HF/Vapor chamber is configured to accept full 4" wafers or smaller samples. Generally, 4" wafers were used in the work described in this thesis. Alcohol and/or water vapor is delivered from heated stainless steel tubes, which are heated up above 100°C to avoid condensation in the tube.

The gas mixture flows through a showerhead and is distributed over the wafer. Process gas is exhausted with a mechanical pump through a liquid nitrogen trap. The base pressure of the chamber is typically on the order of 10^{-7} torr.

2.2 Experimental Procedure

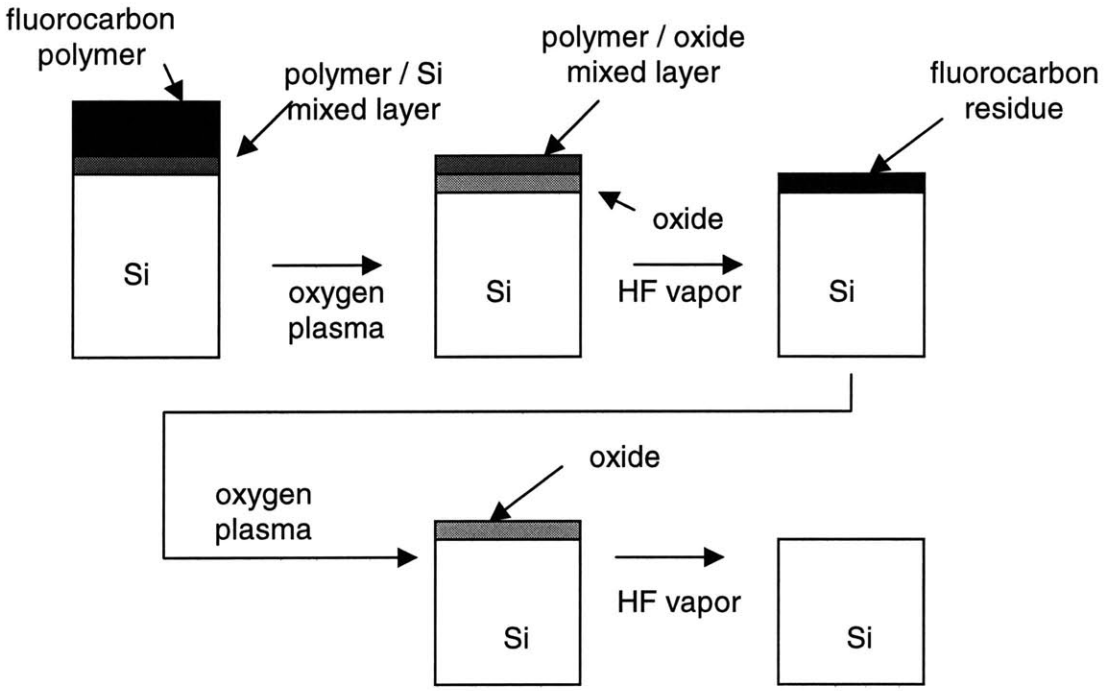

Figure 2.3 A schematic diagram of contaminated/damaged films and the proposde removal procedure.

Figure 2.3 shows proposed schematic diagram of the contaminated films and the removal procedure. After etching the contaminating film consists of a layer of bulk fluorocabon polymer approaching 40 Å in thickness, atop a layer of relatively "clean" SiO_2 approximately 10 thick. At the interface between the polymer and oxide is a transition region of mixed composition, 5-10 Å in thickness. 1st oxygen plasma cleaning removes virtually all of the bulk fluorocarbon film, such that most of the remaining polymer was in a mixed fluorocarbon polymer/oxide environment. 1st HF cleaning strips oxide off

leaving polymer or polymer-like residue on the surface. Another cycle of oxygen plasma and HF vapor cleaning takes care of this to obtain a clean silicon surface.

2.2.1 Etching

100% CHF_3 was used for etching gas with 10sccm flow rate. The reason that we choose this gas composition is 100% CHF_3 is very polymerizing condition forming large amount of polymer after etching, which is good for studying cleaning process. 5500 Å of thermally grown silicon dioxide was used for etching and to build up sufficient amount of polymer, 25% to 100% overetch was performed. RF power of 150 to 200 W were supplied to top coil and 100 to 150 W of bottom power was used. 1.2 kV of DC was applied for the electrostatic chuck. Etch rate was ~ 1500 to 2000 /min.

2.2.2 Oxygen Plasma Cleaning

100% oxygen was used for 1st and 2nd oxygen plasma process. Flow rate was 20 sccm and operating pressure was 35mtorr. RF power of 150 - 200 W was used without bottom RF bias. Processing time was up to 3 minutes.

2.2.3 HF Vapor Cleaning

HF process used in this research was developed by Yong-Pil Han in our group.[22] Figure 2.4 shows the two regimes of HF vapor etching process. In non-condensation regime, the etch rate is in the order of 10s of Å/min, which is two orders of magnitude lower than in condensation regime. By using this process, we were able to strip off the contaminated oxide. The conditions used in this study are as follows: 90°C for sample temperature,

125torr for processing pressure, flow rate of 80sccm for HF, 32sccm for H_2O, 388sccm for N_2. The etch rate under this condition is 8 Å/min and the processing time was ~ 1 minute, which etches 80 Å of oxide.

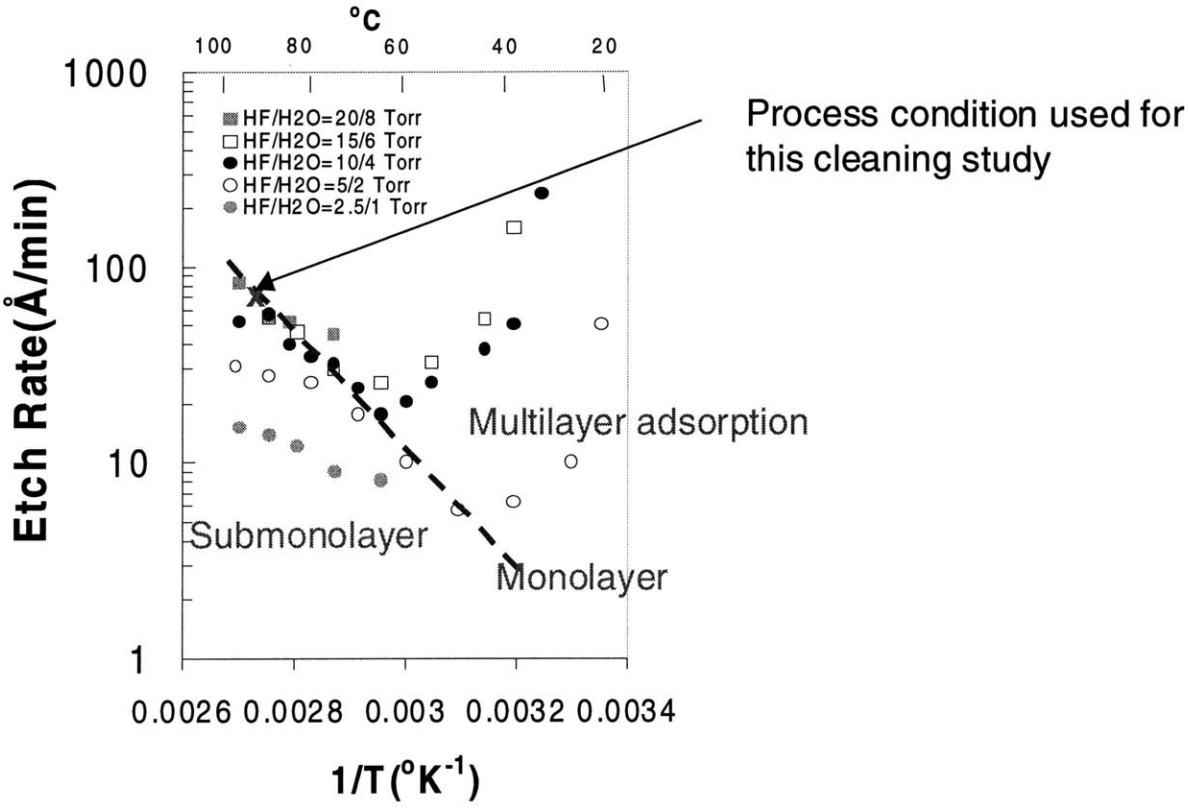

Figure 2.4 Condensation and non-condensation regimes in HF vapor etching.[22]

2.2.4 XPS Analysis

Al Kα was used for X-ray source. Pass energy was 20 V, and number of scans for each element was 50. Take-off angle, which is the angle between detector and the sample was

fixed to 90 degree. All the steady state charge shift was corrected by setting metallic silicon 1s peak to 99.15 eV. Peak height or intensity was normalized with respect to silicon peak area.

Number of monolayer analysis was made as follows.

If the thickness of contamination layer is d, and electron escape depth of the contaminated layer is λ_1 the Si peak intensity from the contaminated sample is

$$I = I_o \exp(-\frac{d}{\lambda_1})$$

where I is Si xps peak intensity from the contaminated film and I_0 is Si xps peak intensity from the clean sample. By comparing I and I_0, we can know d and number of monolayers N is given by

$$N = \frac{d}{d_m}$$

where d_m is monolayer thickness.

Electron escape depth values used in this thesis was 35 Å for Si and SiO_2 and 15 Å for polymeric contamination.[20]

To investigate contamination on trench bottoms and sidewalls, angle resolved XPS was used. Figure 2.5 is a schematic diagram illustrating angle resolved XPS technique.

To see the contamination on trench bottom and top of patterned line the electron detector (analyzer) is placed at 90 degree take-off angle and 25 take-off angle is used to see contamination on sidewalls.

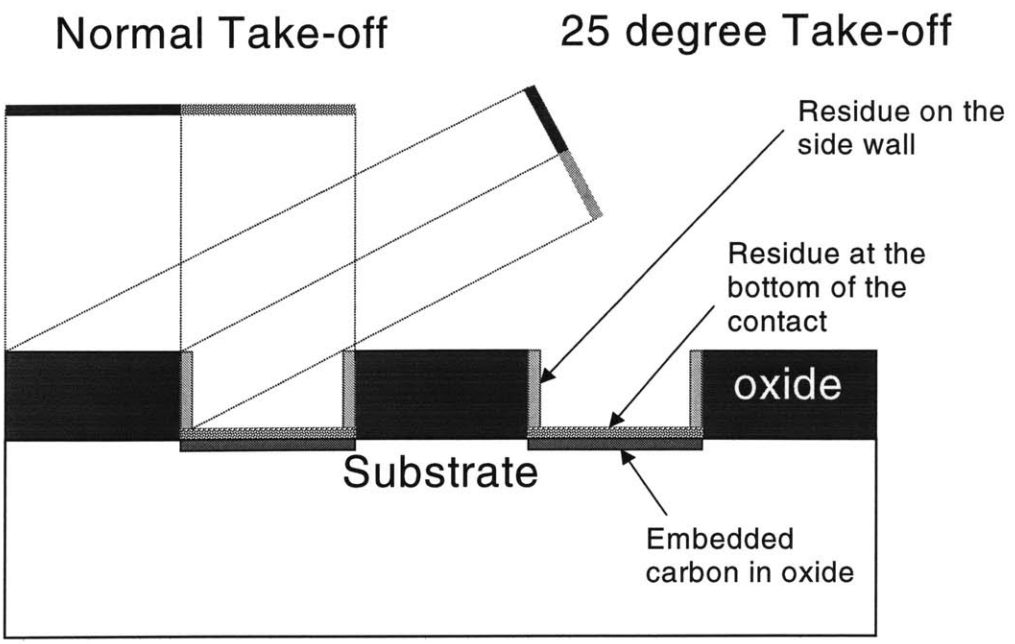

Figure 2.5 A Schematic diagram of angle resolved XPS showing normal take-off angle and 25 degree take-off angle

Chapter 3

Integrated Post Oxide Etch Dry Cleaning

3.1 Removal of Polymeric Contamination from a Planar Surface

For the experiments, 5500 Å thermally grown oxide sample was etched with 25% overetch, and overetching time was about 40 seconds. The etched sample was investigated by using XPS, then processed in oxygen plasma for 3 minutes. HF vapor cleaning was followed, and then oxygen plasma cleaning process and HF vapor cleaning process were repeated.

100% CHF_3 was used for etching gas with 10 sccm flow rate. Operating pressure was 4 mtorr. RF power of 175 W was supplied to top coil and 100 W of bottom power was used. For oxygen plasma, 200 W of top coil power was used without bottom power. 40 mtorr was the pressure and flow rate was 10 sccm. Oxygen plasma cleaning steps were performed for 3 minutes.

Figure 3.1 shows changes in carbon XPS spectra with cleaning steps. In terms of carbon contamination , the sample was cleaned down to detection limit of XPS after oxygen plasma cleaning process. Small carbon peak after each step of HF vapor cleaning process is coming from HF cleaning chamber itself and 'mixed' layer as stated in chapter 1. This small amount of carbon corresponds to ~ 0.5 monolayers, which can be considered as not to be detrimental to electrical contact resistance. Second cycle of oxygen plasma and HF cleaning process does not do anything particular in terms of carbon contamination.

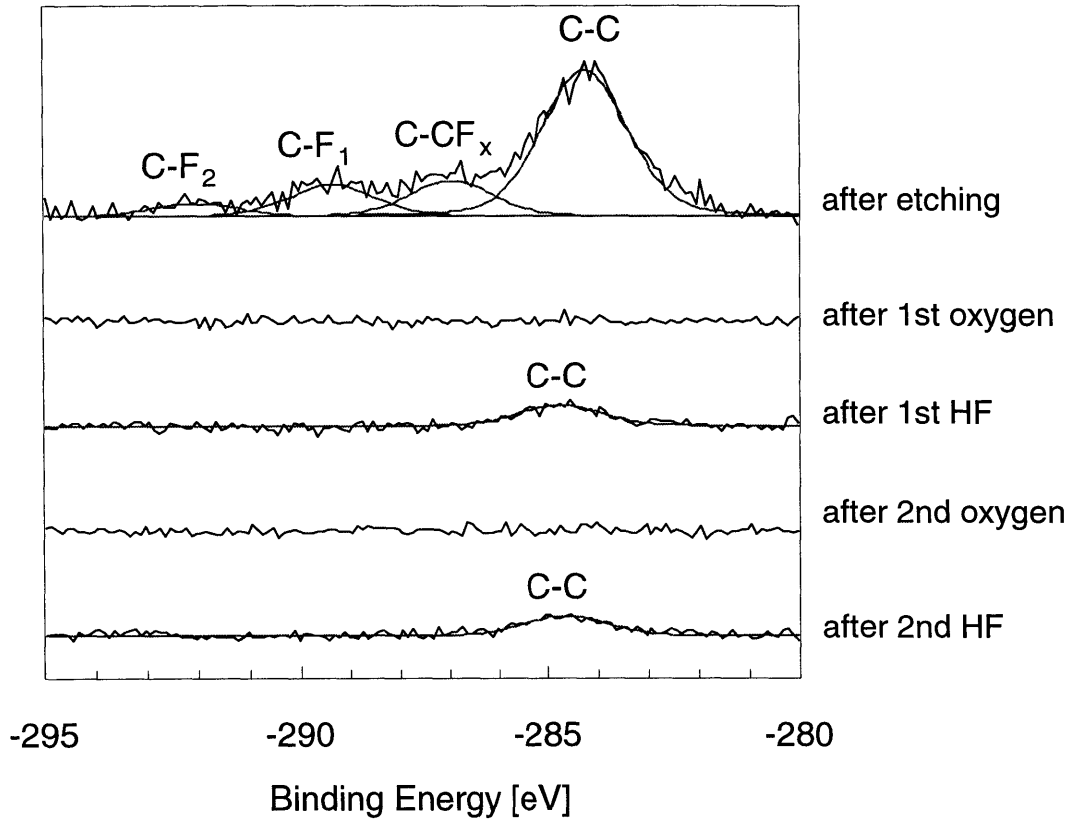

Figure 3.1 Carbon 1s photoelectron emission spectra illustrating oxygen plasma and HF vapor integrated cleaning sequence applied to a blanket oxide film etched at 175 W top / 100 W bottom in 100% CHF_3 at 4 mtorr. Oxygen plasma condition was 200 W top without bottom power in 100% O_2 at 40 mtorr. HF vapor cleaning condition was 20 torr of HF, 8 torr of H_2O and 125 torr of total pressure at 95°C and the processing time was 1 minute.

Figure 3.2 shows changes in silicon XPS spectra with cleaning steps. After etching Si- F_x peak was observed as well as Si-Si peak due to the presence of polymeric contamination on the sample. After 1st oxygen plasma cleaning process, however, Si- F_x peak was not observed. This is because oxygen plasma was successful in oxidizing carbon implanted or carbon imbedded silicon region('mixed' layer) to clean carbons up to form silicon oxide film. No silicon oxide peak was observed, which means there were no Si-O rich layer underneath the fluorocarbon contamination film. This is attributed to the fact that the samples are not exposed to air or oxygen after etching in our integrated cleaning system. HF vapor process strips this oxide off and the second cycle of oxygen plasma cleaning and HF vapor cleaning process makes oxide surface and cleans it up.

Figure 3.3 shows changes in oxygen XPS spectra. After etching, no oxygen peak was observed, which means the sample was completely etched. Oxygen plasma cleaning process forms oxide surface, HF strips it off and the second cycle does the same thing. Small peak shift in samples after oxygen plasma cleaning processes is due to charging shift. Although charging shift was compensated by setting metallic silicon peak (Si-Si) to 99.15 eV, there can be additional charging in the oxide due to its low electrical conductivity.

Figure 3.4 shows Fluorine XPS spectra changes with cleaning processes. Large amount of fluorine which was on the sample in the form of C-F compounds was observed after etching. After oxygen plasma cleaning process, fluorine contamination level was reduced significantly due to the removal of polymeric contamination from the sample. The spectra show that fluorine peaks after oxygen plasma processes are larger than those after HF cleaning processes. This is attributed to resputtered fluorine from the chamber

wall. Although fluorocarbon polymeric film is deposited on the chamber wall which is produced in etching process, carbon can be easily consumed in oxygen plasma when fluorine cannot be.

Small amount of carbon after this cleaning sequence is due to HF chamber contamination, which can be removed by baking HF chamber and small amount of oxygen and fluorine left on the surface can be easily removed by pre-sputter cleaning before metal deposition. So this set of experiments says that the cleaning process is good for removing fluorocabon contamination formed during oxide etch process.

Figure 3.5 summarizes this cleaning sequence and Table 3.1 shows number of monolayers left after each cleaning step for each contaminating element.

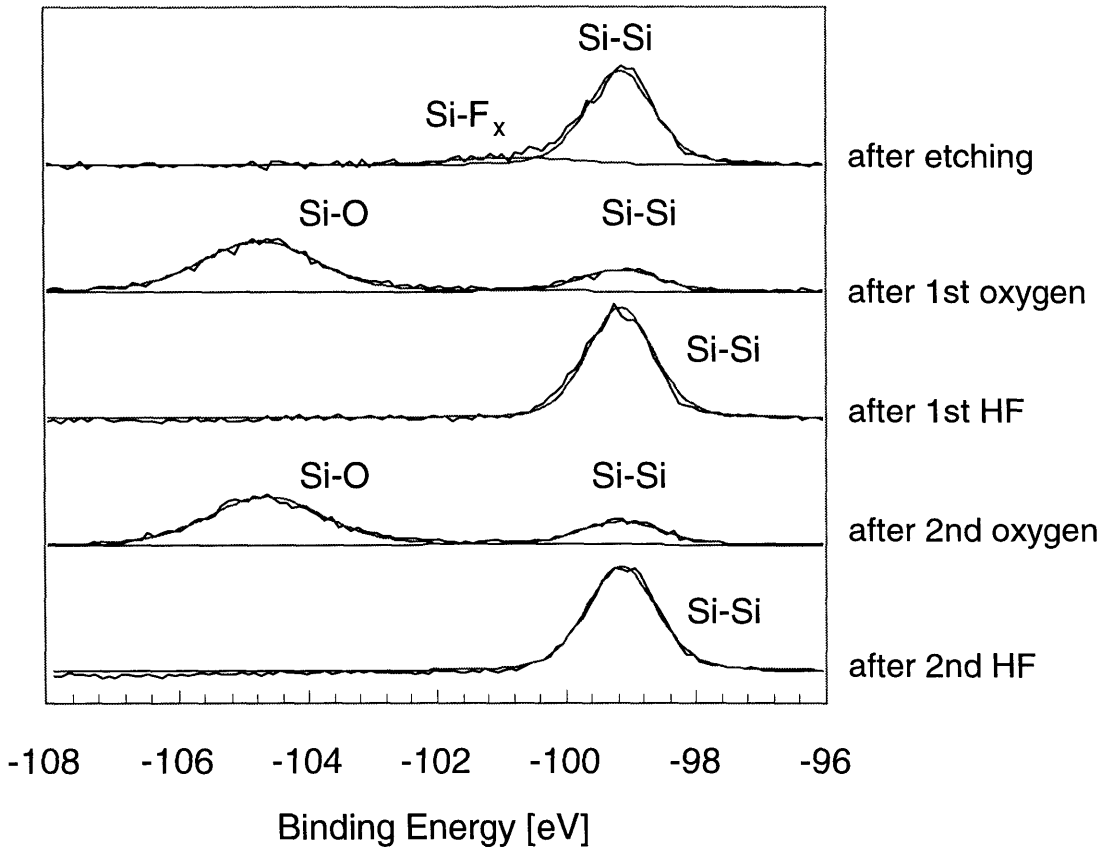

Figure 3.2 Silicon 1s photoelectron emission spectra illustrating oxygen plasma and HF vapor integrated cleaning sequence applied to a blanket oxide film etched at 175 W top / 100 W bottom in 100% CHF_3 at 4 mtorr. Oxygen plasma condition was 200 W top without bottom power in 100% O_2 at 40 mtorr. HF vapor cleaning condition was 20 torr of HF, 8 torr of H_2O and 125 torr of total pressure at 95°C and the processing time was 1 minute.

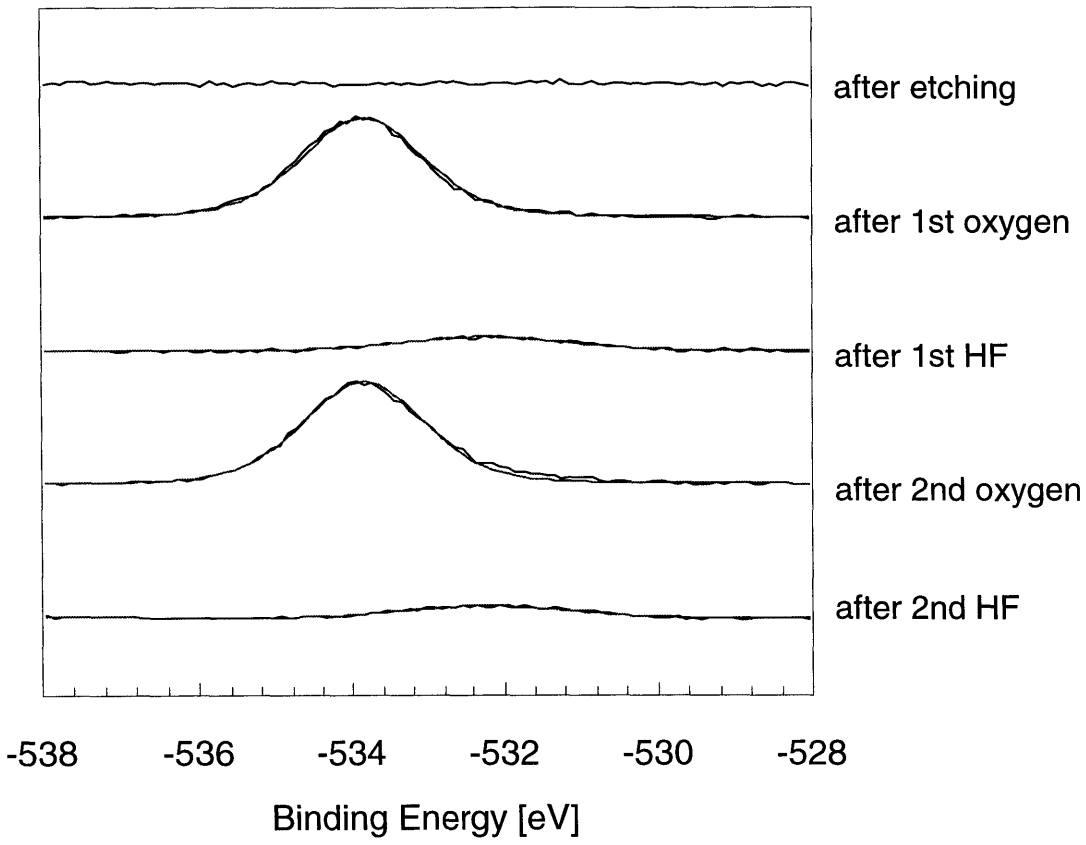

Figure 3.3 Oxygen 1s photoelectron emission spectra illustrating oxygen plasma and HF vapor integrated cleaning sequence applied to a blanket oxide film etched at 175 W top / 100 W bottom in 100% CHF_3 at 4 mtorr. Oxygen plasma condition was 200 W top without bottom power in 100% O_2 at 40 mtorr. HF vapor cleaning condition was 20 torr of HF, 8 torr of H_2O and 125 torr of total pressure at 95°C and the processing time was 1 minute.

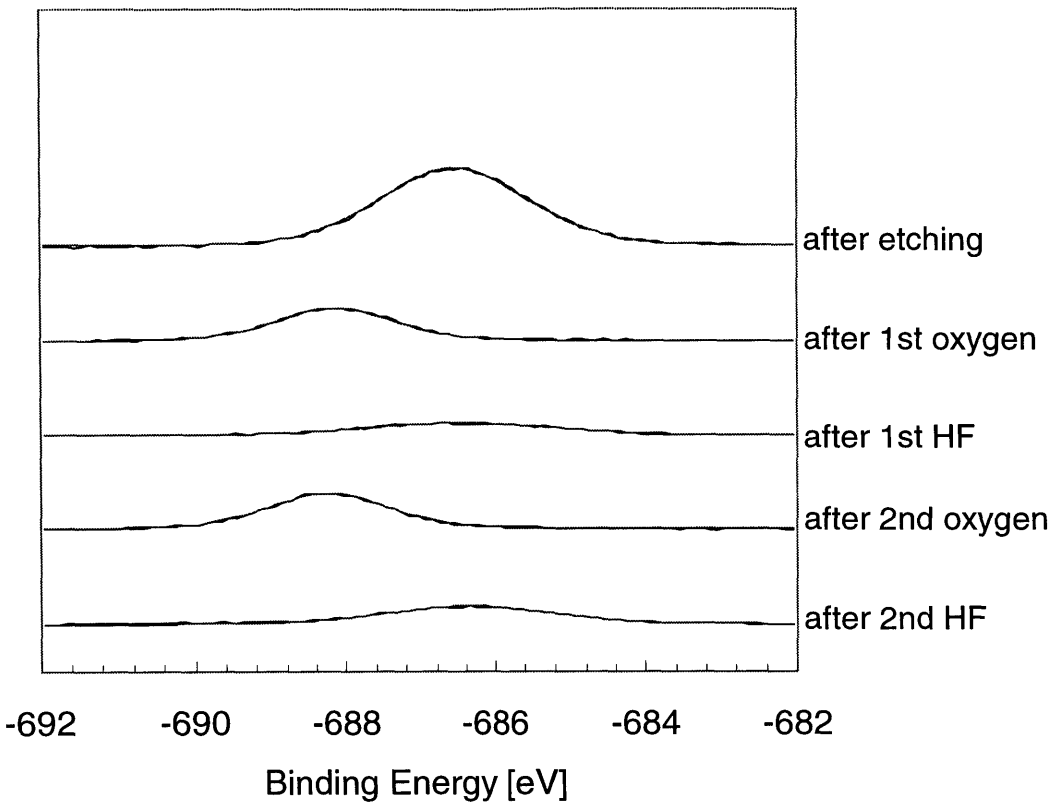

Figure 3.4 Fluorine 1s photoelectron emission spectra illustrating oxygen plasma and HF vapor integrated cleaning sequence applied to a blanket oxide film etched at 175 W top / 100 W bottom in 100% CHF_3 at 4 mtorr. Oxygen plasma condition was 200 W top without bottom power in 100% O_2 at 40 mtorr. HF vapor cleaning condition was 20 torr of HF, 8 torr of H_2O and 125 torr of total pressure at 95°C and the processing time was 1 minute.

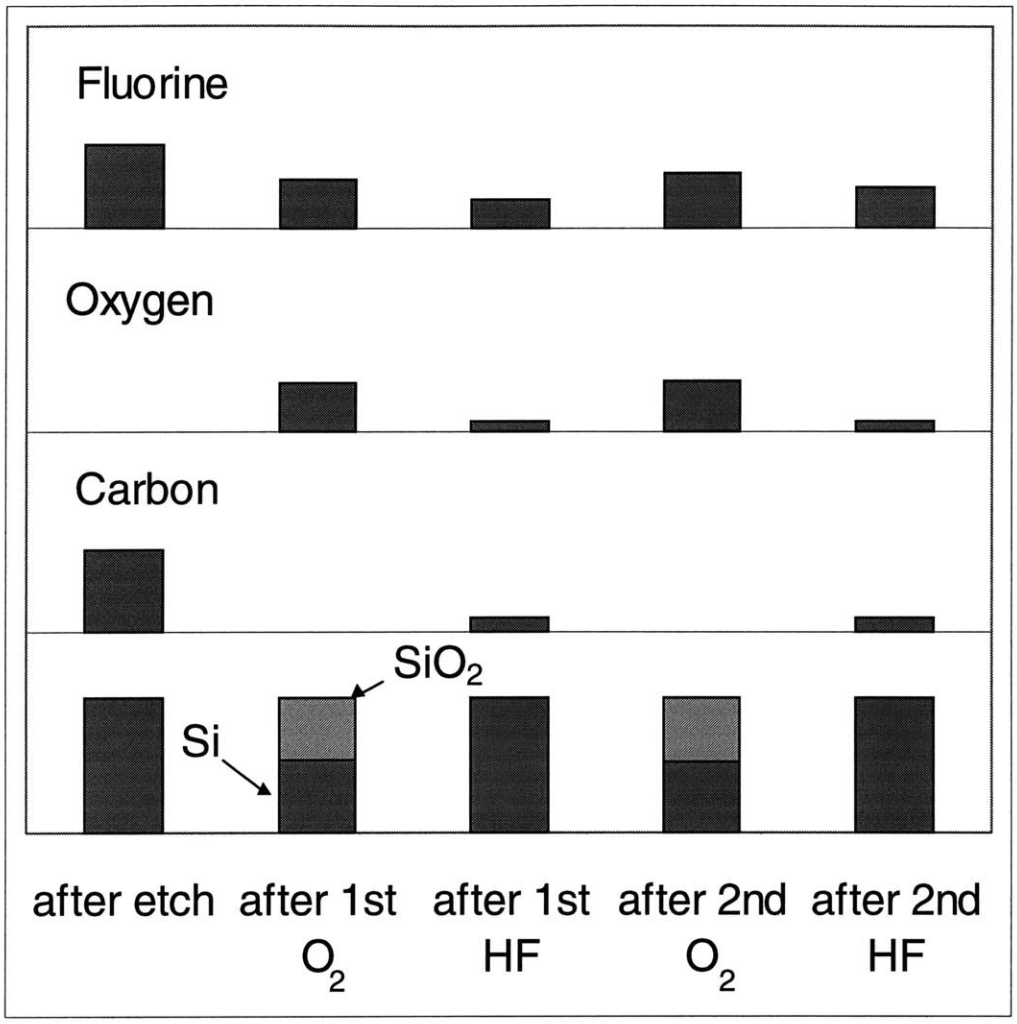

Figure 3.5 A histogram illustrating oxygen plasma and HF vapor integrated cleaning sequence applied to a blanket oxide film etched at 175 W top / 100 W bottom in 100% CHF_3 at 4 mtorr. Oxygen plasma condition was 200 W top without bottom power in 100% O_2 at 40 mtorr. HF vapor cleaning condition was 20 torr of HF, 8 torr of H_2O and 125 torr of total pressure at 95°C and the processing time was 1 minute.

	Carbon	Oxygen	Fluorine
after etching	3.1	0	3.1
after 1st O_2 plasma	0	3.6	1.8
after 1st HF vapor	0.48	0.67	1.1
after 2nd O_2 plasma	0	3.7	2.0
after 2nd HF vapor	0.47	0.73	1.5

Table 3.1 Number of monolayers left after oxygen plasma and HF vapor integrated cleaning sequence applied to a blanket oxide film etched at 175 W top / 100 W bottom in 100% CHF_3 at 4 mtorr. Oxygen plasma condition was 200 W top without bottom power in 100% O_2 at 40 mtorr. HF vapor cleaning condition was 20 torr of HF, 8 torr of H_2O and 125 torr of total pressure at 95°C and the processing time was 1 minute.

3.2 Effect of Etching Condition

In this set of experiment, increased coil power was used to produce less energetic ions during the etching. 200 W of RF power was used for the coil instead of 175 W, which is shown in previous section. Because of this change in etching plasma condition, initial xps carbon peak is pretty different from one in the previous section.

Figure 3.6 shows changes in carbon XPS spectra with cleaning steps. Again, carbon contamination level change shows very similar trend to what we had in the previous section although XPS peak for initial polymeric contamination is different.

Figure 3.7 illustrates silicon XPS spectra changes with cleaning process. This also shows similar behavior to to what we had in the previous section. There is a small Si- F_x peak right after etching, oxide peaks are observed after oxygen plasma cleaning, disappear after HF cleaning.

Figure 3.8 shows changes in oxygen XPS spectra. The changes are again similar to the changes observed in higher energy etching case. Large oxygen peaks are observed after plasma oxygen cleaning, very small oxygen peaks after HF cleaning process.

Figure 3.9 shows changes in fluorine XPS spectra with cleaning process. It is again very similar to one in previous section.

This set of experiments implies that this cleaning process is useful for different kind of polymeric contamination formed in different plasma conditions.

Figure 3.10 summarizes this cleaning sequence and Table 3.2 shows number of monolayers left after each cleaning step for each contaminating element.

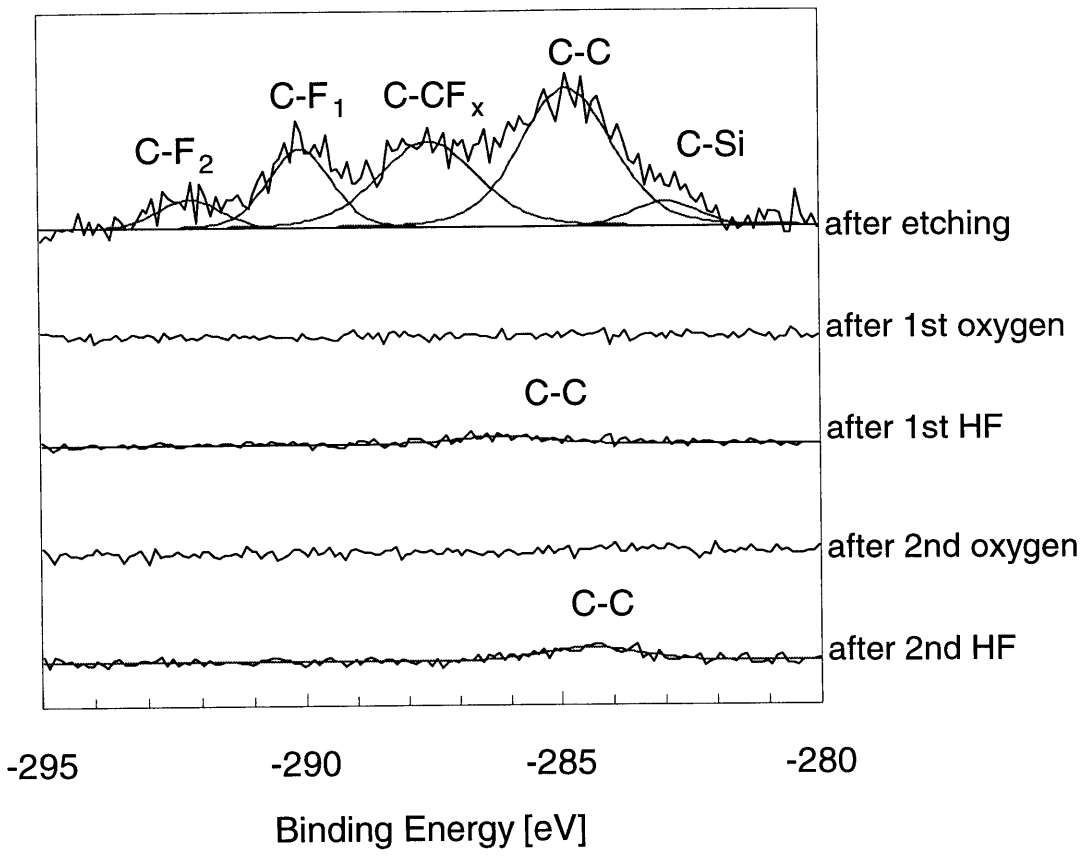

Figure 3.6 Carbon 1s photoelectron emission spectra illustrating oxygen plasma and HF vapor integrated cleaning sequence applied to a blanket oxide film etched at 200 W top / 100 W bottom in 100% CHF_3 at 4 mtorr. Oxygen plasma condition was 200 W top without bottom power in 100% O_2 at 40 mtorr. HF vapor cleaning condition was 20 torr of HF, 8 torr of H_2O and 125 torr of total pressure at 95°C and the processing time was 1 minute.

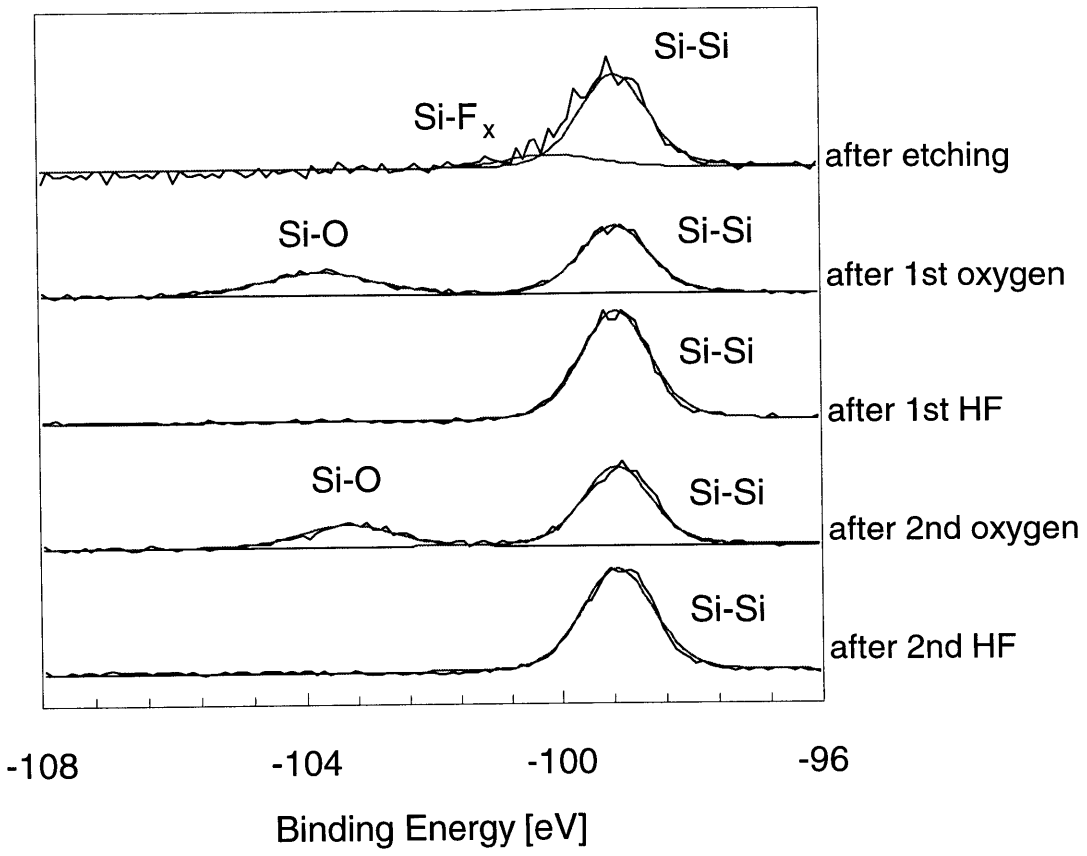

Figure 3.7 Silicon 1s photoelectron emission spectra illustrating oxygen plasma and HF vapor integrated cleaning sequence applied to a blanket oxide film etched at 200 W top / 100 W bottom in 100% CHF_3 at 4 mtorr. Oxygen plasma condition was 200 W top without bottom power in 100% O_2 at 40 mtorr. HF vapor cleaning condition was 20 torr of HF, 8 torr of H_2O and 125 torr of total pressure at 95°C and the processing time was 1 minute.

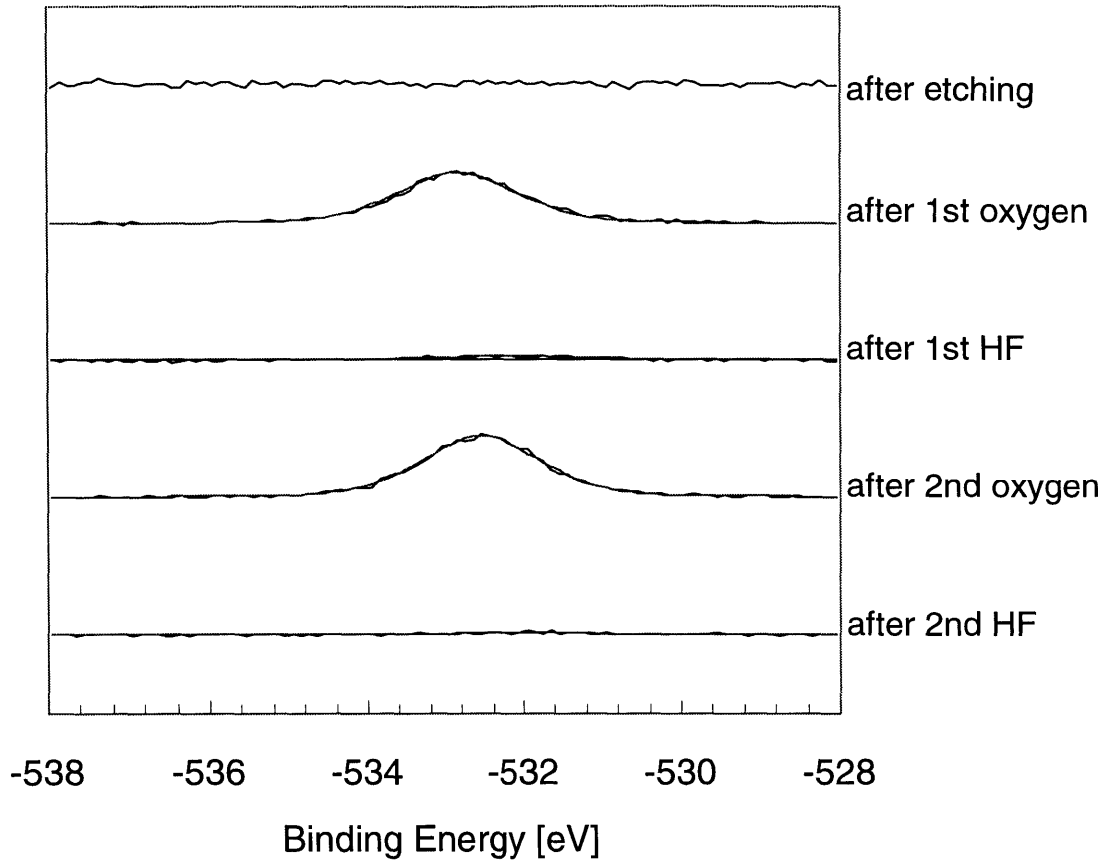

Figure 3.8 Oxygen 1s photoelectron emission spectra illustrating oxygen plasma and HF vapor integrated cleaning sequence applied to a blanket oxide film etched at 200 W top / 100 W bottom in 100% CHF_3 at 4 mtorr. Oxygen plasma condition was 200 W top without bottom power in 100% O_2 at 40 mtorr. HF vapor cleaning condition was 20 torr of HF, 8 torr of H_2O and 125 torr of total pressure at 95°C and the processing time was 1 minute.

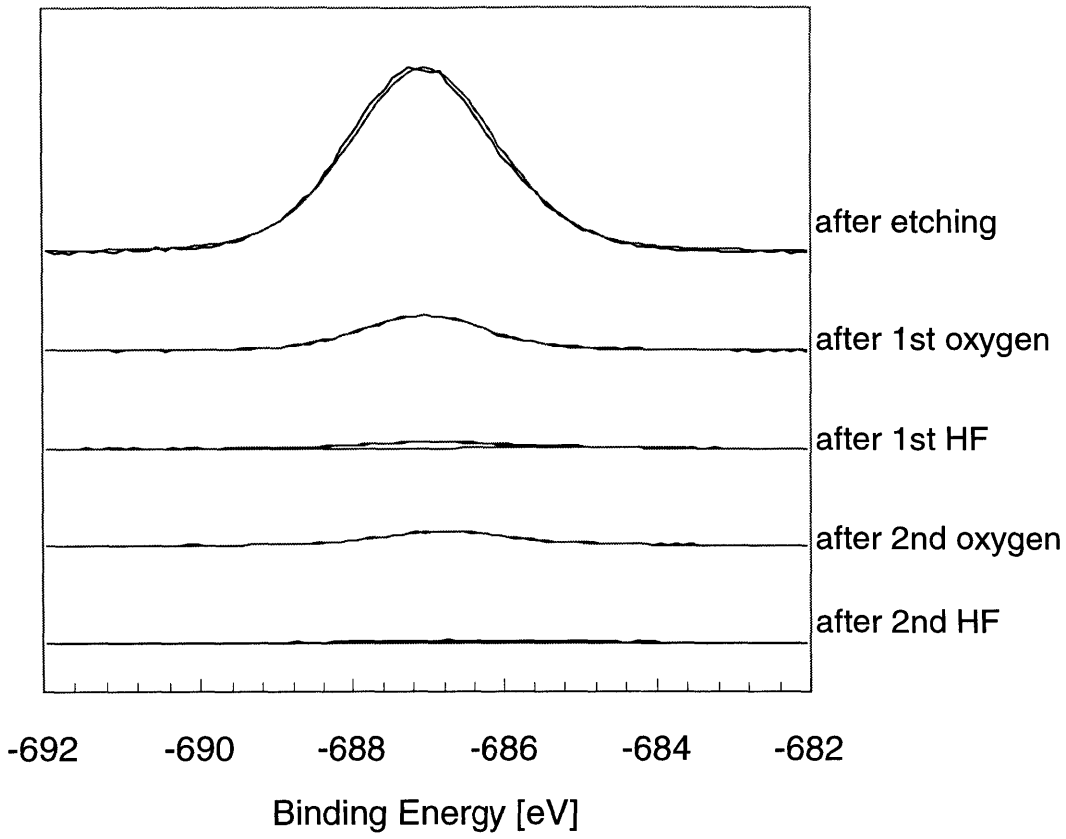

Figure 3.9 Fluorine 1s photoelectron emission spectra illustrating oxygen plasma and HF vapor integrated cleaning sequence applied to a blanket oxide film etched at 200 W top / 100 W bottom in 100% CHF_3 at 4 mtorr. Oxygen plasma condition was 200 W top without bottom power in 100% O_2 at 40 mtorr. HF vapor cleaning condition was 20 torr of HF, 8 torr of H_2O and 125 torr of total pressure at 95°C and the processing time was 1 minute.

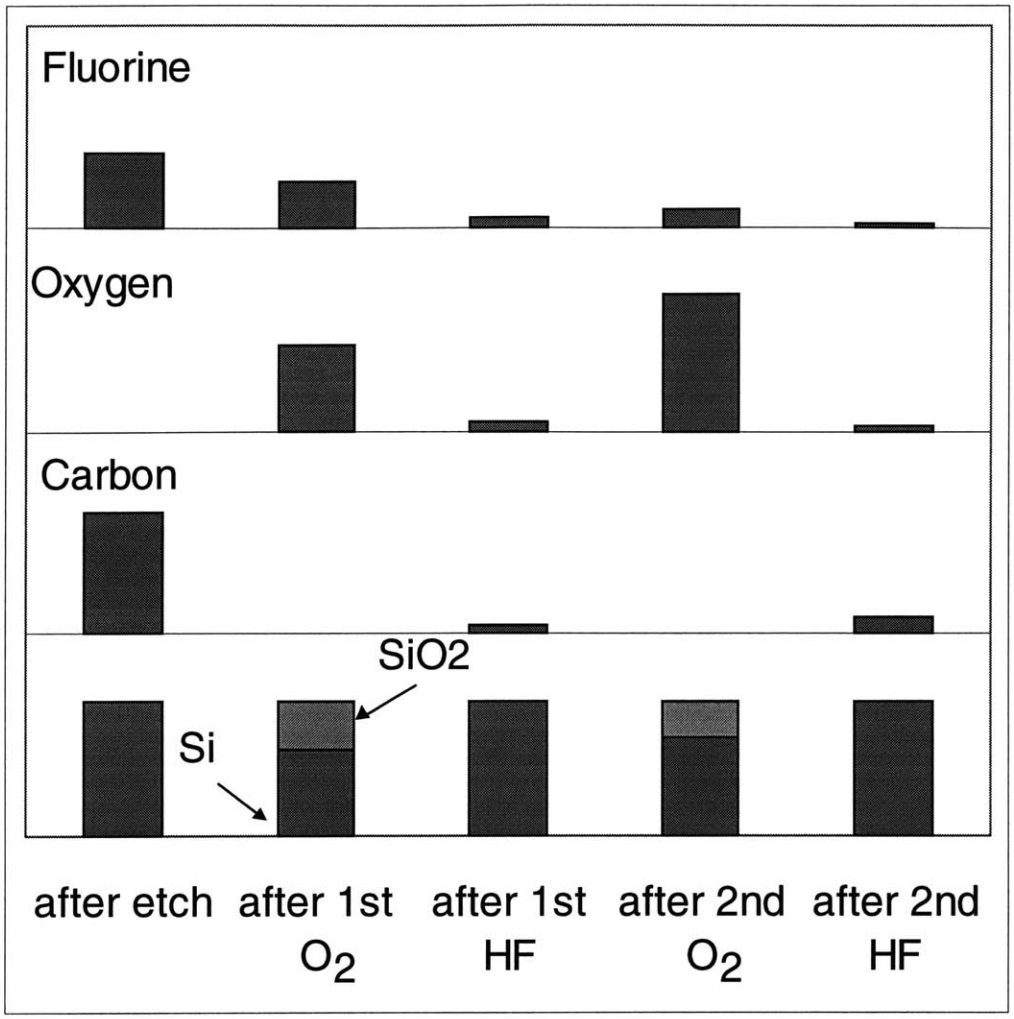

Figure 3.10 A histogram illustrating oxygen plasma and HF vapor integrated cleaning sequence applied to a blanket oxide film etched at 200 W top / 100 W bottom in 100% CHF_3 at 4 mtorr. Oxygen plasma condition was 200 W top without bottom power in 100% O_2 at 40 mtorr. HF vapor cleaning condition was 20 torr of HF, 8 torr of H_2O and 125 torr of total pressure at 95°C and the processing time was 1 minute.

	Carbon	Oxygen	Fluorine
after etching	5.4	0	5.4
after 1st O_2 plasma	0	6.3	3.4
after 1st HF vapor	0.37	0.67	0.73
after 2nd O_2 plasma	0	7.3	1.4
after 2nd HF vapor	0.71	0.36	0.29

Table 3.2 Number of monolayers left after oxygen plasma and HF vapor integrated cleaning sequence applied to a blanket oxide film etched at 200 W top / 100 W bottom in 100% CHF_3 at 4 mtorr. Oxygen plasma condition was 200 W top without bottom power in 100% O_2 at 40 mtorr. HF vapor cleaning condition was 20 torr of HF, 8 torr of H_2O and 125 torr of total pressure at 95°C and the processing time was 1 minute.

3.3 Effect of Spacer under the Coil.

All the results so far are obtained from etcher with 0.5" thick spacer between the coil and the top glass plate to reduce capacitive coupling. Data shown in this section were obtained without 0.5" spacer to see the effect of capacitive coupling.

The experimental conditions used in this set of experiments is same as one in section 3.1. Figure 3.11 shows carbon contamination reduction with the cleaning steps. A lot more amount of carbon is left even after complete set of cleaning process. But as you can see no carbon peak is observed after oxygen plasma cleaning steps. This means something is covering up the carbon peak in this step. This becomes clear when we look at silicon XPS spectra. In Figure 3.12, no metallic silicon peak (Si-Si) is observed after oxygen plasma etching, and even after etching a small amount of silicon oxide is observed. This says that without the spacer, capacitive coupling is so high and the top quartz plate is exposed to fairly high energy ion bombardment to cause sputter deposition from the quartz on the substrate. When we measure the thickness of oxide after oxygen plasma treatment, the thickness is 500-650 Å, which is not reasonable to be considered as plasma grown oxide. For comparison, oxide thickness after oxygen plasma with the spacer is less than 20 Å. Sputter deposited silicon oxide makes it difficult to remove carbon contamination from the sample because it covers the contamination up before oxygen plasma cleans it up.

Without spacers between coil and top quartz plate, cleaning process was not successful in removing polymeric contamination formed during oxide etching.

Figure 3.13 summarizes this cleaning sequence and Table 3.3 shows number of monolayers left after each cleaning step for each contaminating element.

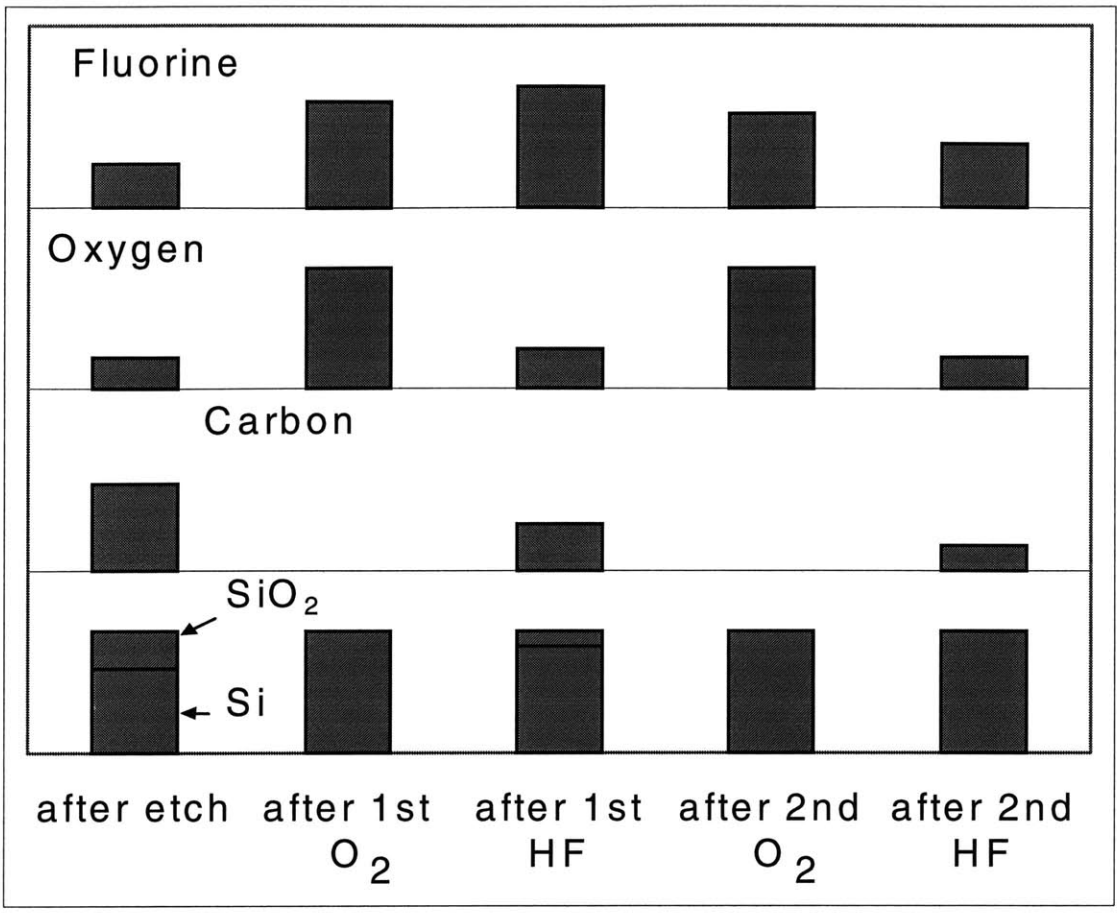

Figure 3.11 Carbon 1s photoelectron emission spectra illustrating oxygen plasma and HF vapor integrated cleaning sequence applied to a blanket oxide film etched at 175 W top / 100 W bottom in 100% CHF_3 at 4 mtorr. Oxygen plasma condition was 200 W top without bottom power in 100% O_2 at 40 mtorr. HF vapor cleaning condition was 20 torr of HF, 8 torr of H_2O and 125 torr of total pressure at 95°C and the processing time was 1 minute. ICP etcher was without teflon spacer between inductive coil and top quartz plate.

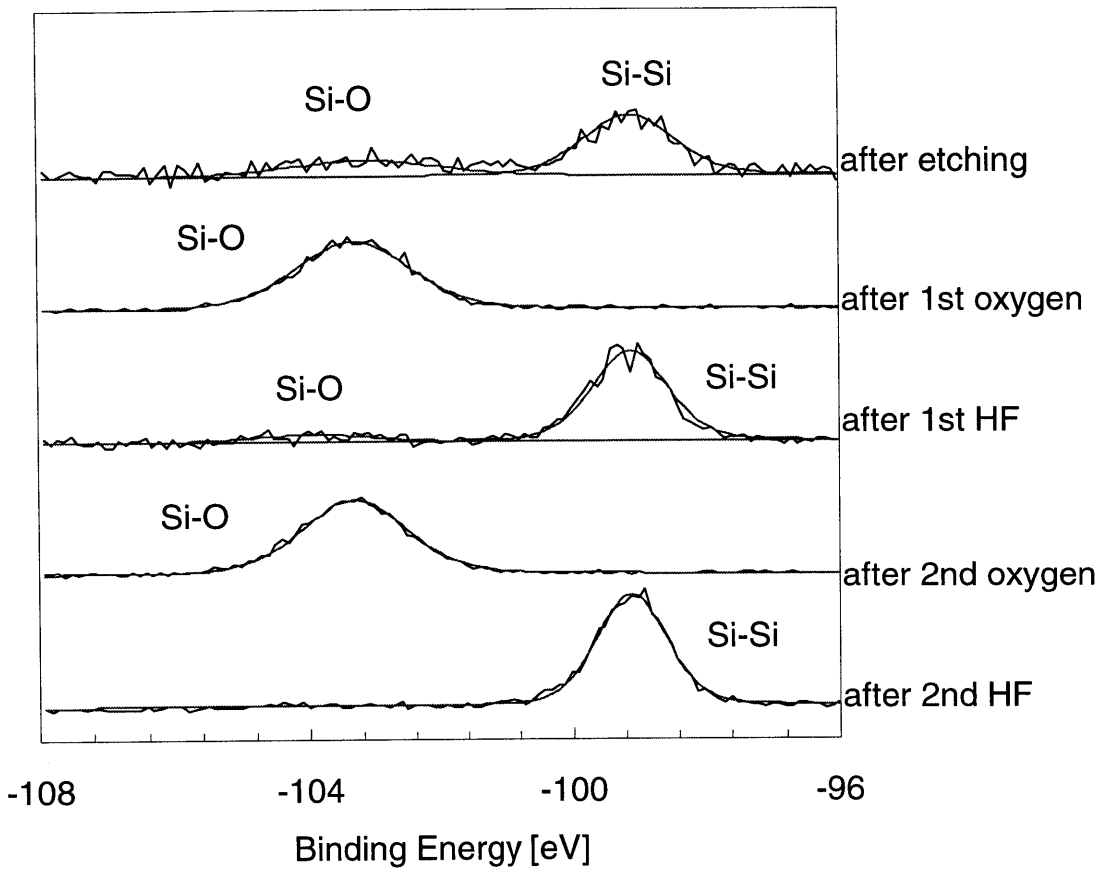

Figure 3.12 Silicon 1s photoelectron emission spectra illustrating oxygen plasma and HF vapor integrated cleaning sequence applied to a blanket oxide film etched at 175 W top / 100 W bottom in 100% CHF_3 at 4 mtorr. Oxygen plasma condition was 200 W top without bottom power in 100% O_2 at 40 mtorr. HF vapor cleaning condition was 20 torr of HF, 8 torr of H_2O and 125 torr of total pressure at 95°C and the processing time was 1 minute. ICP etcher was without teflon spacer between inductive coil and top quartz plate.

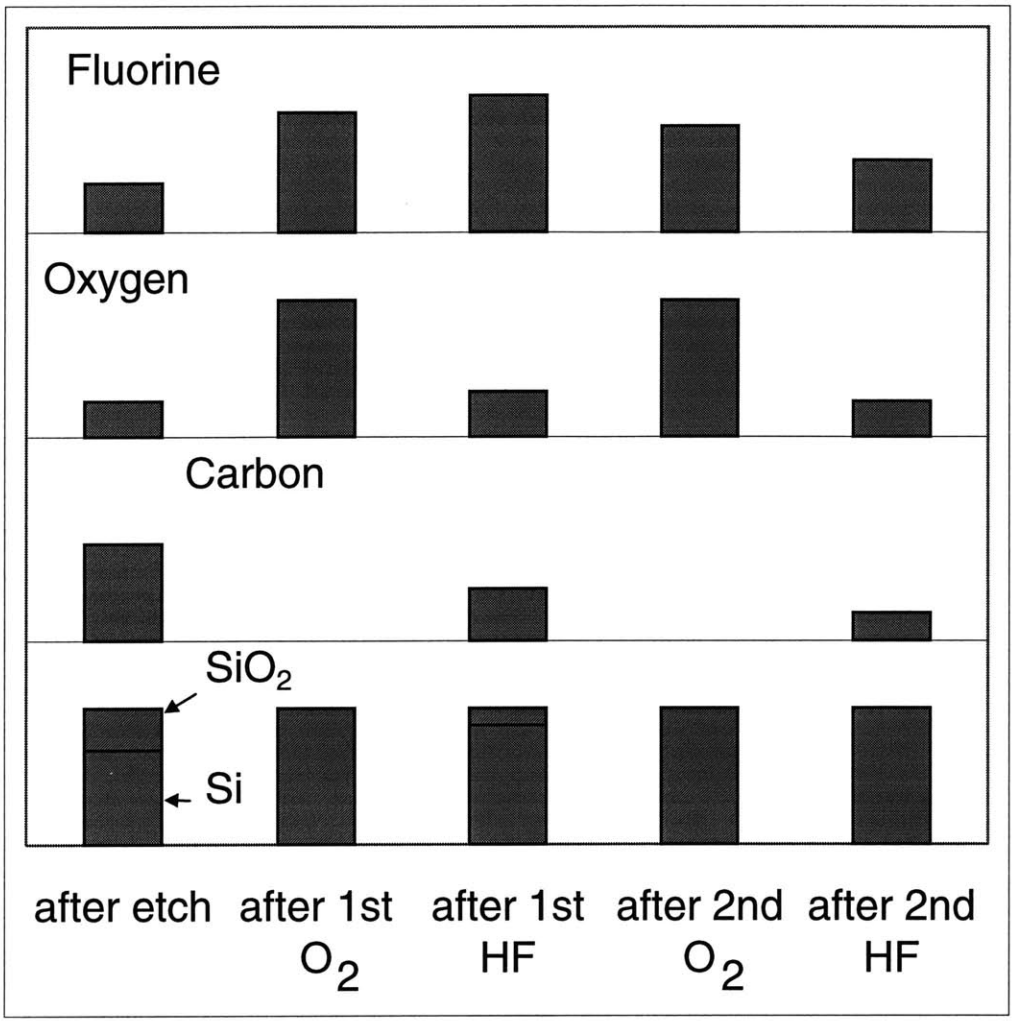

Figure 3.13 A histogram illustrating oxygen plasma and HF vapor integrated cleaning sequence applied to a blanket oxide film etched at 175 W top / 100 W bottom in 100% CHF_3 at 4 mtorr. Oxygen plasma condition was 200 W top without bottom power in 100% O_2 at 40 mtorr. HF vapor cleaning condition was 20 torr of HF, 8 torr of H_2O and 125 torr of total pressure at 95°C and the processing time was 1 minute. ICP etcher was without teflon spacer between inductive coil and top quartz plate.

	Carbon	Oxygen	Fluorine
after etching	7.1	0	7.1
after 1st O_2 plasma	0	thick oxide	17
after 1st HF vapor	3.8	6.6	22
after 2nd O_2 plasma	0	thick oxide	15
after 2nd HF vapor	2.0	5.1	11

Table 3.3 Number of monolayers left after oxygen plasma and HF vapor integrated cleaning sequence applied to a blanket oxide film etched at 175 W top / 100 W bottom in 100% CHF_3 at 4 mtorr. Oxygen plasma condition was 200 W top without bottom power in 100% O_2 at 40 mtorr. HF vapor cleaning condition was 20 torr of HF, 8 torr of H_2O and 125 torr of total pressure at 95°C and the processing time was 1 minute. ICP etcher was without teflon spacer between inductive coil and top quartz plate.

3.4 Removal of Polymeric Contamination from a Line and Space Patterned Sample

The process sequence was also applied to line and space patterned sample. To investigate cleaning process on the trench bottom of the feature as well as the sidewalls, angle resolved x-ray technique was used.

Figure 3.14 illustrates the result of cleaning sequence applied to line and space patterned sample. When this set of experiments were performed, HF chamber was baked to have a cleaner chamber wall, so that there was no carbon contamination from HF chamber itself. After 1st oxygen plasma cleaning process, no carbon was observed from the top, the trench bottom and the sidewall. But after 1st HF vapor cleaning process, small amount of carbon, which corresponds to less than one monolayer. This is 'mixed' layer, which was formed during etching process as mentioned in chapter 2. Since oxide is mixed with fluorocaron polymeric contamination in this layer, it is difficult to be removed by HF vapor cleaning process. 2nd oxygen plasma process step removes 'polymer' portion of this mixed layer and 2nd HF vapor cleaning step removes remaining oxide to have a contamination-free surface. This process was successful in removing contamination from the trench bottom and sidewall.

Figure 3.15 is a SEM photograph showing that this experiment was performed with a vertical sidewall.

Figure 3.16 summarizes this cleaning sequence and Table 3.3 shows number of monolayers left after each cleaning step for each contaminating element.

In Figure 3.16, more fluorine was observed on the sidewalls. This is because sidewalls are exposed to less ion bombardment. But the fluorine contamination level from 25 take-

off angle is less than 1 monolayer, which can be easily removed by pre-sputter cleaning before metal deposition.

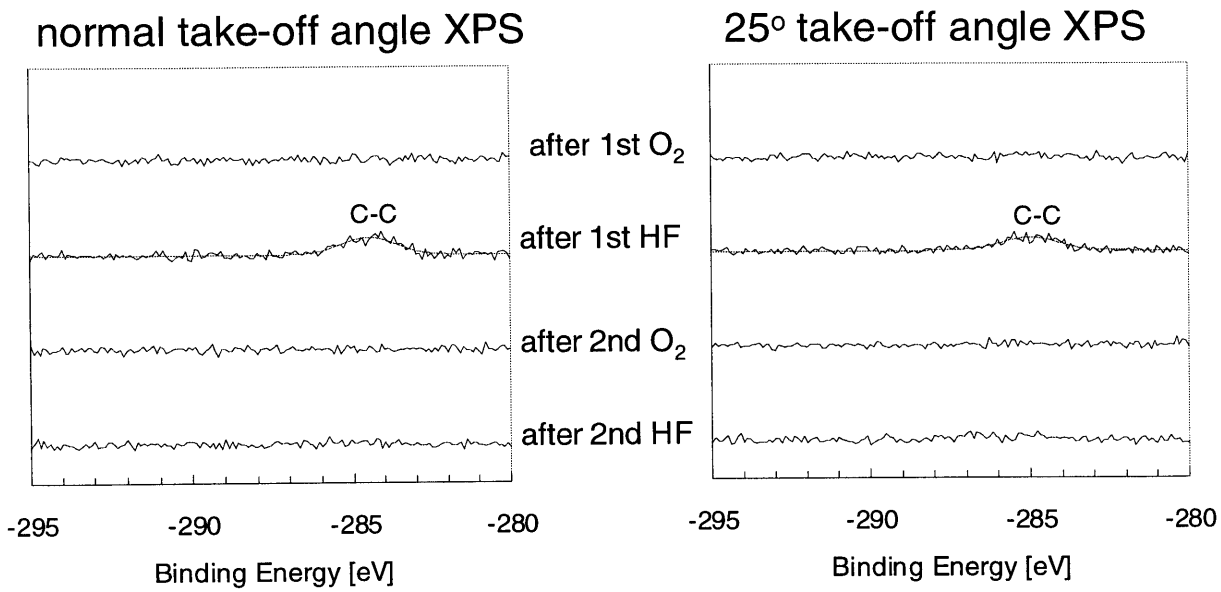

Figure 3.14 Carbon 1s photoelectron emission spectra illustrating oxygen plasma and HF vapor integrated cleaning sequence applied to a line and space patterned sample etched at 200 W top / 100 W bottom in 100% CHF_3 at 4 mtorr. Oxygen plasma condition was 200 W top without bottom power in 100% O_2 at 40 mtorr. HF vapor cleaning condition was 20 torr of HF, 8 torr of H_2O and 125 torr of total pressure at 95°C and the processing time was 1 minute.

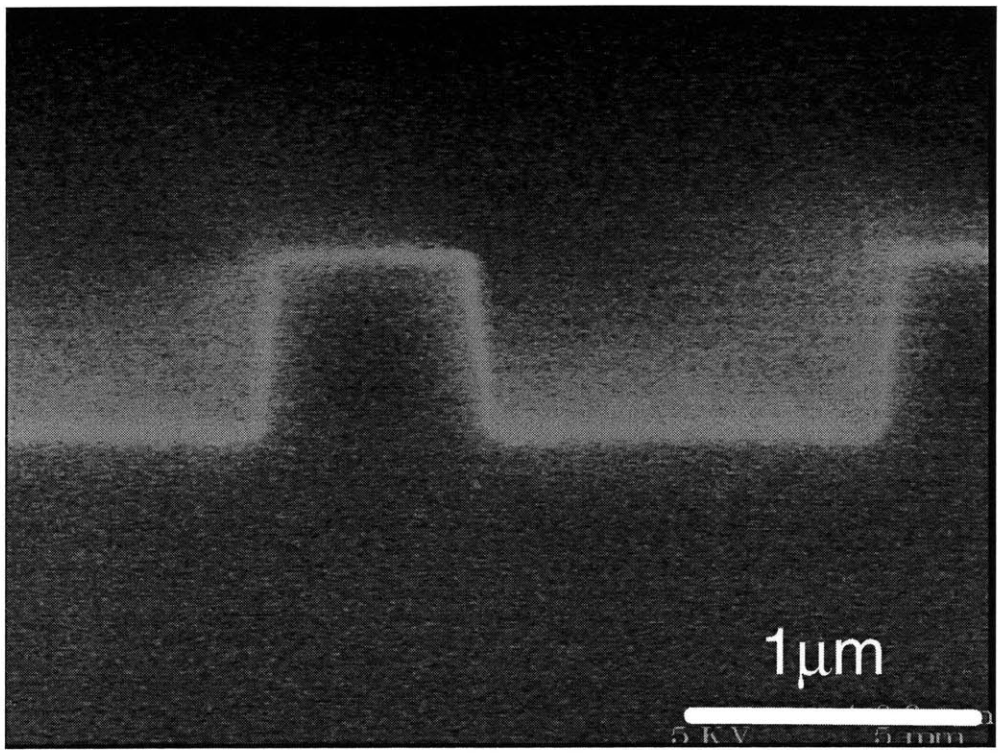

Figure 3.15 SEM photograph showing the etch profile after cleaning sequence. The sidewall angle is 86 degree. line width = 0.7 μm, space width = 1.3 μm

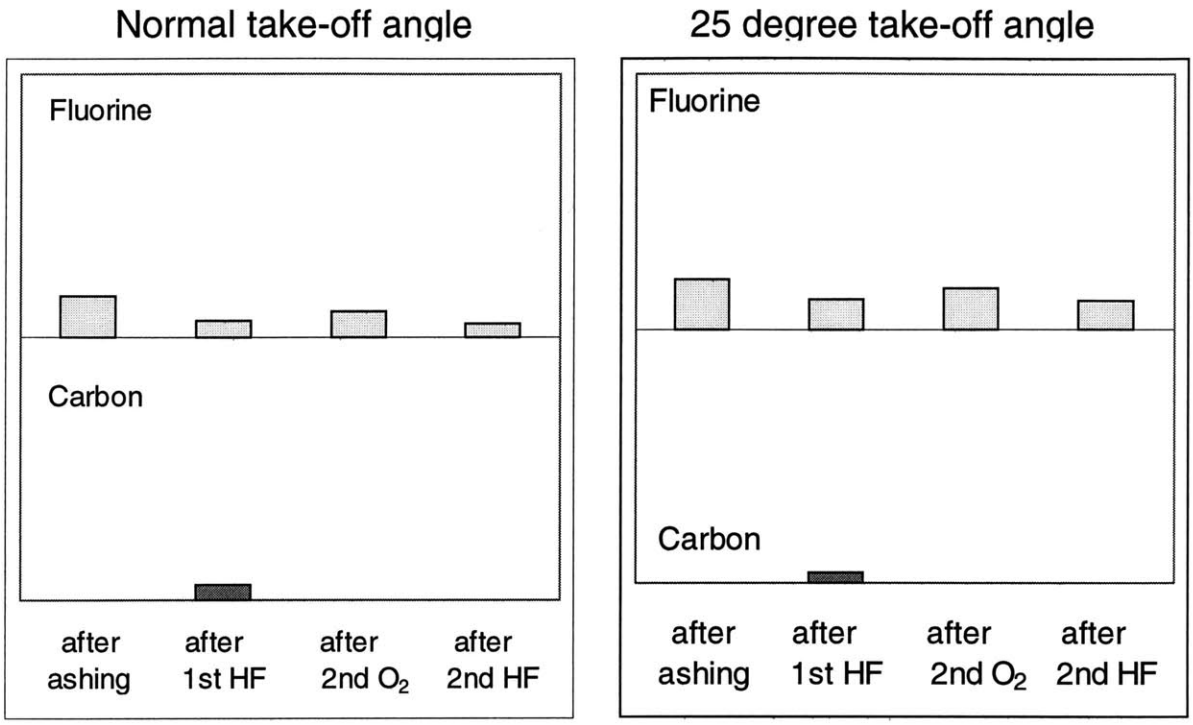

Figure 3.16 A histogram illustrating oxygen plasma and HF vapor integrated cleaning sequence applied to a line and space patterned sample etched at 200 W top / 100 W bottom in 100% CHF_3 at 4 mtorr. Oxygen plasma condition was 200 W top without bottom power in 100% O_2 at 40 mtorr. HF vapor cleaning condition was 20 torr of HF, 8 torr of H_2O and 125 torr of total pressure at 95°C and the processing time was 1 minute

	normal take-off angle		25 take-off angle	
	carbon	fluorine	carbon	fluorine
after ashing	0	1.2	0	1.5
after 1st HF vapor	0.44	0.5	0.34	0.9
after 2nd O_2 plasma	0	0.8	0	1.3
after 2nd HF vapor	0	0.4	0	0.9

Table 3.4 Number of monolayers left after oxygen plasma and HF vapor integrated cleaning sequence applied to a line and space patterned sample etched at 200 W top / 100 W bottom in 100% CHF_3 at 4 mtorr. Oxygen plasma condition was 200 W top without bottom power in 100% O_2 at 40 mtorr. HF vapor cleaning condition was 20 torr of HF, 8 torr of H_2O and 125 torr of total pressure at 95°C and the processing time was 1 minute.

Chapter 4

Conclusions

Experiments on integrated post oxide etch cleaning process have been performed, with oxygen plasma cleaning process and HF vapor cleaning process with blanket oxide films. The results indicate that removing polymeric contamination which is formed during oxide etching process can be removed by using oxygen plasma - HF vapor - oxygen plasma - HF vapor process sequence. The integrated process worked very well to remove polymeric contamination formed under high ion energy etching condition and under low ion energy etching condition. Spacer between RF top coil and top quartz plate played an important role in reducing sputter deposition from top plate by reducing capacitive coupling.

Chapter 5

References

1. J. W. Coburn, *Journal of Applied Physics* **50**, 5210 (1979).

2. G. S. Oehrlein, Y. Zhang, D. Vender, M. Haverlag, *Journal of Vacuum Science and Techology* **A12**, 323 (1994).

3. G. S. Oehrlein, Y. Zhang, D. Vender, O. Joubert, *Journal of Vacuum Science and Technology* **A12**, 333 (1994).

4. H. Shan, B. K. Srinivasan, J. D. W. Jillie, J. S. Multani, W. J. Lo, *Journal of Electrochemical Society* **141**, 2904 (1994).

5. Y. Wang, S. W. Graham, L. Chan, S. Loong, *Journal of Electrochemical Society* **144**, 1522 (1997).

6. H. H. Sawin, *Microelectronic Engineering* **23**, 15-21 (1994).

7. M. Lieberman, R. Gottscho, , *"Design of High Density Plasma Sources for Materials Processing*. J. Vossen, Ed., Advances in Res. and Dev. (Academic Press, Orlando, FL, 1993), vol. 17.

8. J. H. Keller, J. C. Forster, M. S. Barnes, *J. Vac. Sci. Technol. A* **10**, 3426 (1992).

9. J. Hopwood, C. R. Guarnieri, S. J. Whitehair, J. J. Cuomo, *J. Vac. Sci. Technol. A* **11**, 147 (1993).

10. O. Joubert, G. S. Oehrlein, M. Surendra, *Journal of Vacuum Science and Technology* **A12**, 665 (1994).

11. O. Joubert, G. S. Oehrlein, Y. Zhang, *Journal of Vacuum Science and Technology* **A12**, 658 (1994).

12. T. Ono, R. Hamasaki, T. Mizutani, *Japanese Journal of Applied Physics* **33**, L171 (1994).

13. J. W. Coburn, *Plasma Etching and Reactive Ion Etching* (1982).

14. J. W. Coburn, *Journal of Vacuum Science and Technology* **A12**, 1417 (1994).

15. G. S. Oehrlein, R. M. Tromp, J. C. Tsang, Y. H. Lee, E. J. Petrillo, *Journal of Electrochemical Society* **132**, 1441-1447 (1985).

16. G. J. Coyle, G. S. Oehrlein, *Applied Physics Letter* **47**, 604-606 (1985).

17. J. H. Thomas, X. C. Mu, S. J. Fonash, *Journal of Electrochemical Society* **134**, 3122-3125 (1987).

18. G. S. Oehrlein, *Journal of Vacuum Science and Technology* **A11**, 34-46 (1993).

19. A. S. Yapsir, G. Fortuno-Wiltshire, J. P. Gambino, R. H. Kastl, P. C. C, *Journal of Vacuum Science and Technoogy* **A8**, 2939-2944 (1990).

20. G. E. Muilenberg, *Handbook of X-ray Photoelectron Spectroscopy* (Perkin-Elmer Corporation, Eden Prairie, MN, 1979).

21. J. W. Coburn, H. F. Winters, *Journal of Vacuum Science and Technology* **16**, 391-403 (1979).

22. Y.-P. Han, A. S. Lawing, H. H. Sawin, *Proceedings of the Fifth International Symposium on Cleaning Technology in Semiconductor Device Manufacturing. Electrochemical Society* , 423-430 (1998).